

“Lens” Effect in Directed Assembly of Nanowires on *Gradient* Molecular Patterns

Sung Myung,[†] Jiwoon Im,[†] Ling Huang,[‡] Saleem G. Rao,[§] Taekyeong Kim,[†]
Dong Joon Lee,[†] and Seunghun Hong^{*,†}

School of Physics and NANO Systems Institute, Seoul National University, Seoul 151-747, Korea,
Department of Chemistry, Northwestern University, Evanston, Illinois 60208, U.S.A., and Department of
Physics, Florida State University, Tallahassee, Florida 32306, U.S.A.

Received: April 5, 2006; In Final Form: April 27, 2006

We report a new phenomenon, named here as the “lens” effect, in the directed-assembly process of nanowires (NWs) on self-assembled monolayer (SAM) patterns. In this process, the adsorption of NWs is focused in the *nanoscale* regions at the center of *microscale* SAM patterns with *gradient* surface molecular density just like an optical lens focuses light. As a proof of concepts, we successfully demonstrated the massive assembly of V₂O₅ NWs and single-walled carbon nanotubes (swCNTs) with a *nanoscale* resolution using only *microscale* molecular patterning methods. This work provides us with important insights about the directed-assembly process, and from a practical point of view, it allows us to generate nanoscale patterns of NWs over a large area for mass fabrication of NW-based devices.

Recently, there has been much attention given to new devices based on various nanowires (NWs) such as V₂O₅ NWs and ZnO NWs and carbon nanotubes (CNTs).^{1–9} However, a major stumbling block holding back their practical applications can be the lack of a massive assembly method for such devices. Several successful fabrication methods include catalyst pattern-directed growth,¹⁰ the flow cell method,¹¹ capillary-force-driven assembly,^{12,13} and dielectrophoresis.¹⁴ On the other hand, direct interactions between NWs and self-assembled monolayer (SAM) patterns have been utilized to direct the large-scale assembly of NWs on solid substrates.^{8,15–17} However, the resolution of the directed-assembly method is still limited by that of SAM patterning methods, and one often has to rely on slow serial nanolithography techniques for molecular patterning to control individual NWs. Thus, it is still very difficult to prepare nanoscale patterns of NWs over a large surface area for practical applications. Herein, we report a new phenomenon which is named here as the “lens” effect in the sense that SAM patterns with *gradient* surface molecular density *focus* the NW assembly to the center of the patterns just like an optical lens focuses the lights. In this case, the adsorption of NWs is focused in the *nanoscale* regions at the center of *microscale* SAM patterns while leaving the remaining area empty. We can observe the similar effect from both V₂O₅ NWs and single-walled carbon nanotubes (swCNTs) even though they interact with SAM patterns via quite different interaction forces. This result implies that the “lens” effect can be a general phenomenon in directed-assembly processes driven by the direct interactions between NWs and SAM patterns. As a proof of concepts, we demonstrated the directed assembly of V₂O₅ NWs and swCNTs with

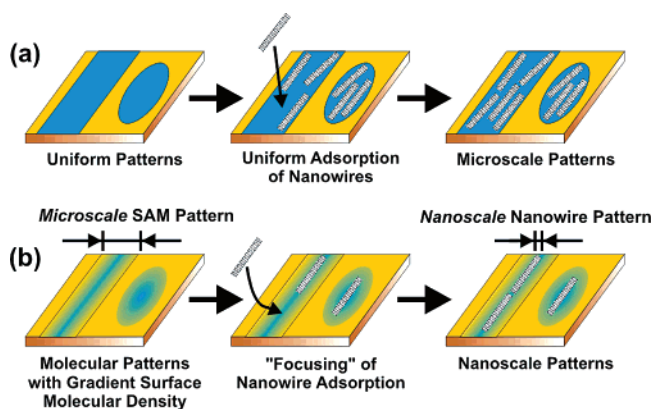


Figure 1. Schematic diagram depicting the directed assembly of V₂O₅ NWs and swCNTs onto (a) *uniform* molecular patterns and (b) *gradient* molecular patterns. In the case of gradient molecular patterns, the assembly of NWs is focused to the *nanoscale* regions at the center of the *microscale* SAM patterns, resulting in *nanoscale* patterns of NWs.

a nanoscale resolution over a large surface area using only microscale molecular patterning methods such as microcontact printing. This work provides us with important insights about the directed-assembly process of NWs, and from a practical point of view, it allows us to easily generate nanoscale patterns of NWs over a large surface area for mass fabrication of NW-based devices such as field effect transistors, interconnection, and chemical or biological sensors.^{1–9}

Figure 1 shows a schematic diagram comparing the *normal* directed-assembly process of NWs (Figure 1a) with the *lens* effect (Figure 1b). At first, SAM patterns with *uniform* or *gradient* molecular density were generated on solid substrates via microcontact printing (MCP)^{18,19} or dip-pen nanolithography (DPN).^{20–23} Here, amine-terminated cysteamine SAM was utilized to direct the adsorption of both V₂O₅ NWs and swCNTs on Au substrates, while we utilized 1-octadecanethiol (ODT)

* Corresponding author. Phone: +82-2-880-1343. Fax: +82-2-884-3002.
E-mail: shong@phya.snu.ac.kr.

[†] Seoul National University.

[‡] Northwestern University.

[§] Florida State University.

SAM to block the NW adsorption.^{8,15} We utilized DPN to generate small-size patterns for the initial process development. However, all SAM patterns in this manuscript were generated via MCP, and they cover an $\sim 1\text{ cm} \times 1\text{ cm}$ area on Au surfaces. Uniform SAM patterns comprised of cysteamine and ODT SAM regions can be generated by first stamping ODT SAM for $\sim 8\text{ s}$ and then backfilling the remaining area with cysteamine (Supporting Information). If one stamps ODT for a relatively longer time ($\sim 16\text{ s}$ in our experiments), ODT molecules laterally diffuse out between the stamped regions and generate submonolayer SAM regions with gradually decreasing ODT density (Supporting Information).¹⁸ Then, the regions with gradient ODT density are backfilled with cysteamine, eventually resulting in mixed SAM regions with gradient cysteamine molecular density. Previous reports also show that submonolayer or mixed SAM patterns can be generated via various other methods including DPN²² and deposition from a mixture of different inks.²⁴ In the mixed SAM regions, the surface molecular density of amine-terminated cysteamine molecules has the maximum value at the center of the regions and decreases slowly as it approaches the boundary.

We can utilize atomic force microscope (AFM) topography and lateral force microscope (LFM) images to distinguish between *uniform* and *gradient* SAM patterns. In the AFM topography images, the cysteamine SAM region appears as a darker area than the ODT SAM regions because of the shorter chain length of cysteamine molecules. If the molecular densities of both cysteamine and ODT SAMs are uniform, the height should change abruptly on the boundary between the two SAM regions, resulting in *sharp* edges of the SAM patterns in AFM topography (Supporting Information). On the other hand, we can observe a *blurred* boundary in the case of *gradient* SAM patterns (Supporting Information). Under ambient conditions, LFM images were reported to represent the hydrophobicity of the surfaces.¹⁹ Hydrophilic surfaces such as cysteamine SAMs appear as brighter areas than hydrophobic ODT SAMs. We can also observe the blurred boundary in the LFM images of *gradient* SAM patterns (inset of Figure 3d).

When the patterned substrate is placed in the solution of V_2O_5 NWs or swCNTs (for usually $\sim 10\text{ s}$), both V_2O_5 NWs and swCNTs are attracted to cysteamine SAM regions.^{8,15–17} We utilized V_2O_5 NW solution prepared by the procedure as reported before.⁸ We prepared the swCNT suspension in dichlorobenzene with 0.5 mg/mL concentration unless otherwise specified.¹⁵ On *uniform* SAM patterns, V_2O_5 NWs and swCNTs assemble uniformly over the cysteamine patterns, while, in the case of *gradient* SAM patterns, V_2O_5 NWs and swCNTs are driven toward the center of the mixed SAM regions where the surface density of cysteamine has a maximum value.

Parts a and b of Figure 2 show the assembly of V_2O_5 NWs onto *uniform* and *gradient* SAM patterns, respectively. The NWs are found to assemble uniformly over uniform cysteamine patterns on Au surfaces (Figure 2a). Previous reports show that V_2O_5 NWs are usually negatively charged in the solution, and they are attracted to the SAMs with positively charged terminal groups such as amine. The results of V_2O_5 NW adsorption onto the mixed SAM regions with gradient cysteamine density are quite surprising (Figure 2b). Even though the mixed SAM regions with amine-terminated cysteamine molecules extend over $2\text{ }\mu\text{m}$ wide line-shaped regions (dark area), the adsorption of V_2O_5 NWs is literally *focused* in the 80 nm wide regions at the center. Presumably, the negatively charged V_2O_5 NWs are driven toward the center of the mixed SAM regions where the positive charge density is maximum due to the high density of

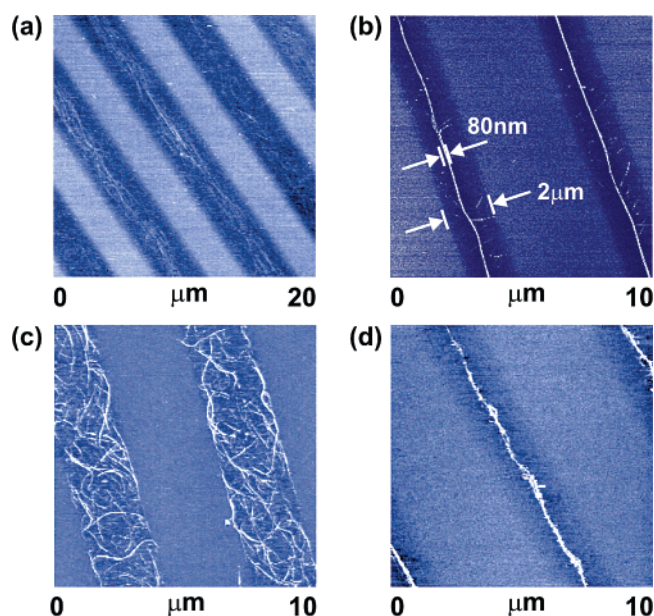


Figure 2. AFM topography images of V_2O_5 NWs and swCNTs on various SAM patterns: (a) V_2O_5 NWs on uniform patterns comprised of ODT (bright area) and cysteamine (dark area); (b) V_2O_5 NWs on the mixed SAM regions with gradient cysteamine surface molecular density on Au (ODT is utilized for passivation); (c) swCNTs on uniform cysteamine SAM patterns on Au; (d) swCNTs on gradient cysteamine patterns on Au. These patterns cover a large surface area ($\sim 1\text{ cm} \times 1\text{ cm}$) on the substrates.

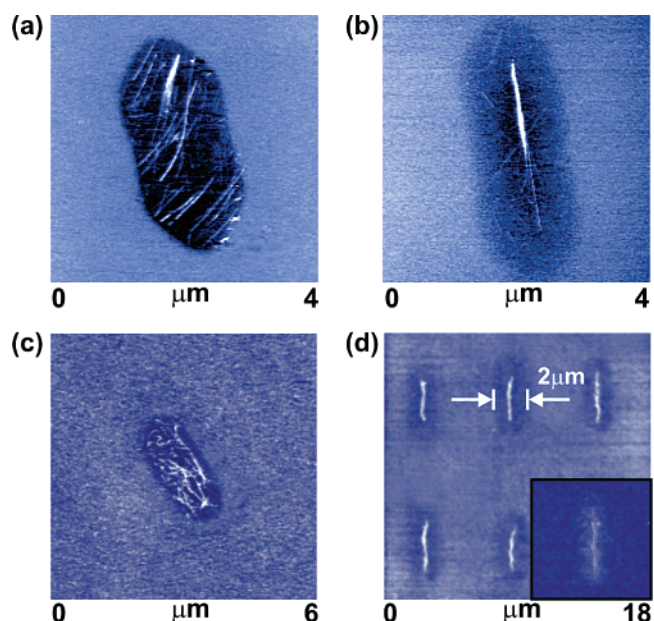


Figure 3. Directed assembly of V_2O_5 NWs and swCNTs on elliptical-shaped molecular patterns. AFM topography images of V_2O_5 NWs on (a) uniform cysteamine SAM patterns and (b) cysteamine SAM patterns with gradient surface molecular density on Au substrates. AFM topography images of swCNTs on (c) uniform cysteamine SAM patterns and (d) SAM patterns with gradient surface molecular density. ODT is utilized for passivation. In the AFM topography images, the cysteamine SAM region appears as a darker area than the ODT SAM regions. The inset of part d shows the lateral force microscope image ($7\text{ }\mu\text{m} \times 7\text{ }\mu\text{m}$) of swCNTs assembled onto an elliptical-shaped gradient SAM pattern. The hydrophilic cysteamine regions appear as a brighter area than the hydrophobic ODT SAM. These patterns cover a large surface area ($\sim 1\text{ cm} \times 1\text{ cm}$) on Au substrates.

amine-terminated cysteamine molecules. It should be noted that NW adsorption is *well-focused* at the center of the mixed SAM regions even though other areas in the regions also have some

positive charges. This result clearly demonstrates the efficiency of this phenomenon. We also would like to mention that these patterns cover a large surface area ($\sim 1\text{ cm} \times 1\text{ cm}$) on the substrates.

We can also observe a similar phenomenon from the directed assembly of swCNTs. swCNTs are reported to be attracted to polar surface regions.¹⁵ Here, SAM patterns with amine-terminal groups can be utilized as a polar surface to direct the adsorption of swCNTs. On uniform cysteamine patterns, swCNTs form uniform patterns as reported in previous works (Figure 2c).¹⁵ However, on the mixed SAM patterns with gradient surface density, the adsorption of swCNTs is focused to the center of the cysteamine patterns, and we can even control the swCNT adsorption down to a few-swCNTs level (Figure 2d). A plausible explanation can be that swCNTs are driven to the center of the patterns, where the polarization is maximum, to minimize the interface energies between swCNTs and surfaces. Some of the previous reports showed swCNT adsorption experiments driven by capillary forces, where droplets of swCNT solution are captured via polar SAM patterns.¹² However, this is not the case of our experiments because we dipped entire patterned substrates in the swCNT solution without using droplets of swCNT solution. This strategy allowed us to easily generate nanoscale lines of swCNTs over a large surface area ($\sim 1\text{ cm} \times 1\text{ cm}$).

We can use elliptical-shaped SAM patterns to control the locations and alignment of adsorbed NWs over a large surface area (Figure 3). Parts a and c of Figure 3 show uniform patterns of V_2O_5 NWs and swCNTs adsorbed on uniform cysteamine regions, respectively. NWs are adsorbed uniformly on the cysteamine regions without crossing over to the nonpolar ODT regions. On the other hand, when we use the SAM patterns with gradient surface molecular density, we can precisely control the adsorption and alignment of V_2O_5 NWs and swCNTs down to a few-NWs level (Figure 3b and d). Figure 3b shows several V_2O_5 NWs *focused* at the center of the elliptical-shaped cysteamine patterns with gradient molecular density. Please note the “blurred” boundary due to the gradual change of cysteamine surface density. We can also control the adsorption of swCNTs down to a few-swCNTs level (Figure 3d). It should be noted that even though the shape of molecular patterns in Figure 3d is similar to that in Figure 3c, swCNTs are adsorbed only in the nanoscale regions at the center of the microscale molecular patterns while leaving the remaining area empty. One important control parameter in this assembly process can be the concentration of swCNT suspensions.¹⁵ In general, we can reduce the number of adsorbed swCNTs by using low concentration swCNT suspensions. For example, when we dip *uniform* elliptical-shaped SAM patterns in a low concentration swCNT suspension ($\sim 0.01\text{ mg/mL}$) for a short time period ($\sim 3\text{ s}$), we can assemble even a single swCNT onto a uniform microscale pattern (Supporting Information). However, the swCNT assembly is not focused to the center of the patterns, and the swCNT was adsorbed at a random location on the uniform patterns. The result implies that it is essential to use *gradient* SAM patterns to achieve the lens effect even though the concentration of swCNT suspension can be utilized to control the number of adsorbed swCNTs down to a few-swCNTs level.

In summary, we report the observation of the lens effect during the directed-assembly process of NWs, where *microscale*

mixed SAM patterns with gradient surface molecular density *focus* the adsorption of NWs in the *nanoscale* regions at the center of the SAM patterns just like an optical lens focuses the lights. We can observe a similar effect for both V_2O_5 NWs and swCNTs even though their interaction forces with SAM surfaces are quite different. This result implies that this effect can be a general phenomenon and can be utilized as a general means to control the directed assembly of NWs down to an individual NW level. As a proof of concepts, we successfully demonstrated the assembly of nanoscale patterns of V_2O_5 NWs and swCNTs over a large surface area utilizing only microscale patterning tools such as stamping.

Acknowledgment. This project has been supported by KOSEF through NRL and TND programs. S.H. acknowledges the partial support from MOCIE.

Supporting Information Available: A method to generate amine-terminated cysteamine patterns with uniform or gradient surface molecular density and swCNT assembly results using the swCNT suspensions with various concentrations. This material is available free of charge via the Internet at <http://pubs.acs.org>.

References and Notes

- (1) Dai, H.; Hafner, J. H.; Rinzler, A. G.; Colbert, D. T.; Smalley, R. E. *Nature* **1996**, *384*, 147.
- (2) Baughman, R. H.; Cui, C.; Zakhidov, A.; Iqbal, Z.; Barisci, J.; Spinks, G.; Wallace, G.; Mazzoldi, A.; Rossi, D.; Rinzler, A.; Jaschinski, O.; Roth, S.; Kertesz, M. *Science* **1999**, *284*, 1340.
- (3) Bachtold, A.; Hadley, P.; Nakanishi, T.; Dekker, C. *Science* **2001**, *294*, 1317.
- (4) de Heer, W. A.; Ch  telain, A.; Ugarte, D. *Science* **1995**, *270*, 1179.
- (5) Martel, R.; Schmidt, T.; Shea, H. R.; Hertel, T.; Avouris, Ph. *Appl. Phys. Lett.* **1998**, *73*, 2447.
- (6) Frank, S.; Poncharal, P.; Wang, Z. L.; de Heer, W. A. *Science* **1998**, *280*, 1744.
- (7) Rueckes, T.; Kim, K.; Joselevich, E.; Tseng, G. Y.; Cheung, C. L.; Lieber, C. M. *Science* **2000**, *289*, 94.
- (8) Myung, S.; Lee, M.; Kim, G. T.; Ha, J. S.; Hong, S. *Adv. Mater.* **2005**, *17*, 2361.
- (9) Guo, J.; Goasguen, S.; Lundstrom, M.; Datta, S. *Appl. Phys. Lett.* **2002**, *81*, 1486.
- (10) Kong, J.; Soh, H. T.; Cassell, A. M.; Quate, C. F.; Dai, H. *Nature* **1998**, *395*, 878.
- (11) Huang, Y.; Duan, X.; Wei, Q.; Lieber, C. M. *Science* **2001**, *291*, 630.
- (12) Wang, Y.; Maspoch, D.; Zou, S.; Schatz, G.; Smalley, R.; Mirkin, C. A. *Proc. Natl. Acad. Sci. U.S.A.* **2006**, *103*, 2026.
- (13) Oh, S. J.; Cheng, Y.; Zhang, J.; Shimoda, H.; Zhou, O. *Appl. Phys. Lett.* **2003**, *82*, 2521.
- (14) Krupke, R.; Hennrich, F.; L  hneysen, H. V.; Kappes, M. M. *Science* **2003**, *301*, 344.
- (15) Rao, S. G.; Huang, L.; Setyawati, W.; Hong, S. *Nature* **2003**, *425*, 36.
- (16) Liu, J.; Casavant, M.; Cox, M.; Walters, D.; Boul, P.; Lu, W.; Rimberg, A.; Smith, K.; Colbert, D.; Smalley, R. *Chem. Phys. Lett.* **1999**, *303*, 125.
- (17) Hannon, J. B.; Afzali, A.; Klinke, Ch.; Avouris, Ph. *Langmuir* **2005**, *21*, 8569.
- (18) Xia, Y.; Whitesides, G. M. *J. Am. Chem. Soc.* **1995**, *117*, 3274.
- (19) Wilbur, J. L.; Biebuyck, H. A.; MacDonald, J. C.; Whitesides, G. M. *Langmuir* **1995**, *11*, 825.
- (20) Piner, R. D.; Zhu, J.; Xu, F.; Hong, S.; Mirkin, C. A. *Science* **1999**, *283*, 661.
- (21) Namjav, D.; Ivanisevic, A. *Adv. Mater.* **2003**, *15*, 1805.
- (22) Sheehan, P. E.; Whitman, L. J. *Phys. Rev. Lett.* **2002**, *88*, 156104.
- (23) Coffey, D. C.; Ginger, D. S. *J. Am. Chem. Soc.* **2005**, *127*, 4564.
- (24) Bain, C. D.; Whitesides, G. M. *Langmuir* **1989**, *5*, 1370.